JGP Journal of General Physiology

COMMENTARY

Progress in understanding slow inactivation speeds up

Jian Payandeh

Voltage-gated sodium (Nav) channels are highly specialized for their essential roles in electrical signaling. Nav channels undergo rapid activation to initiate the rising phase of the action potential, followed by fast and slow inactivation processes (Ahern et al., 2016). Fast inactivation attenuates inward Na^+ conductance on the millisecond time scale, allowing cells to repolarize and Nav channels to become available for reactivation. Upon prolonged or high frequency depolarizations, slow inactivation, which occurs over second to minute timescales, regulates cellular excitability by reducing the number of Nav channels available for activation. Nav channels subjected to longer depolarizing or higher frequency pulses will require more time at negative potentials to recover (Vilin and Ruben, 2001; Silva, 2014). Therefore, slow inactivation encodes molecular memory of previous excitation and contributes to slow spike adaptation and action potential burst termination (Vilin and Ruben, 2001; Silva, 2014). Slow inactivation is clinically relevant because local anesthetic, anti-arrhythmic, and anti-epileptic drugs have the highest affinity for slow inactivated Nav channels (Vilin and Ruben, 2001; Silva, 2014). Subtle defects in slow inactivation can cause disease, including mutations associated with periodic paralysis and Brugada syndromes (Vilin and Ruben, 2001). Although the molecular correlates governing Na^+ selectivity, voltage-dependent activation, and fast inactivation have been well studied (Ahern et al., 2016), the structural basis of slow inactivation in Nav channels has remained enigmatic. A study in the *Journal of General Physiology* applied electron paramagnetic resonance (EPR) spectroscopy methods to a model bacterial Nav (BacNav) channel in order to shed light on the process of slow inactivation (see Chatterjee et al., in this issue), just in time to commemorate 95 years since the physiological relevance of the phenomenon was first recognized (Woronzow, 1924).

Eukaryotic Nav (eNav) channels are functionally and architecturally asymmetric. The pore-forming subunit is comprised of four homologous domains (DI–DIV) linked together in a single polypeptide (Fig. 1 A), where four voltage-sensing domains (VSD1–4) surround a central ion-conducting pore module (PM; Yan et al., 2017). Upon membrane depolarization, voltage-dependent activation of VSD1-VSD3 couples through the S4-S5 linkers to dilate the S6 activation gate and initiate Na^+ conductance. Fast inactivation strictly requires VSD4 activation, but can occur from open or closed channel states (Capes et al., 2013). The fast inactivation gating particle is located within the intracellular DIII-DIV linker (Fig. 1 A) and was proposed to occlude the central S6 conduction pathway through a hinged-lid mechanism (Kellenberger et al., 1996). Structural studies have since identified a more peripheral S6 receptor site and postulated an allosteric mechanism of fast inactivation (Yan et al., 2017). Either way, protease removal of the fast inactivation gating particle, or directed mutation to the crucial IFM (isoleucine-phenylalanine-methionine) motif, completely incapacitates fast inactivation but leaves slow inactivation intact (Armstrong et al., 1973; West et al., 1992). These clues indicate that the mechanisms underlying the processes of slow inactivation are distinct from fast inactivation and are localized to other regions of the Nav channel structure.

Available evidence suggests that the PM and selectivity filter regions of Nav channels are involved in slow inactivation gating. Mutations within and around the pore-helix 1 (P1) and pore-helix 2 (P2)-loops, including known pathogenic mutations, affect slow inactivation (Vilin and Ruben, 2001; Silva, 2014). Low external Na^+ concentrations accelerate entry into the slow inactivated state, whereas high external Na^+ concentrations or tetrodotoxin (TTX) binding to the selectivity filter impede slow inactivation (Townsend and Horn, 1997; Cervenka et al., 2010). A conceptual link with C-type inactivation in potassium channels has therefore been suggested, but other Nav channel regions have been implicated in slow inactivation, including the VSDs, indicating that these are distinct gating phenomena (Vilin and Ruben, 2001; Silva, 2014). The modulated receptor hypothesis for drug block within the central cavity stipulates that slow inactivation in Nav channels must involve a conformational change that includes rearrangement of the PM (Hille, 1977). However, the mechanisms

Department of Structural Biology, Genentech, Inc..

Correspondence to Jian Payandeh: payandeh.jian@gene.com.

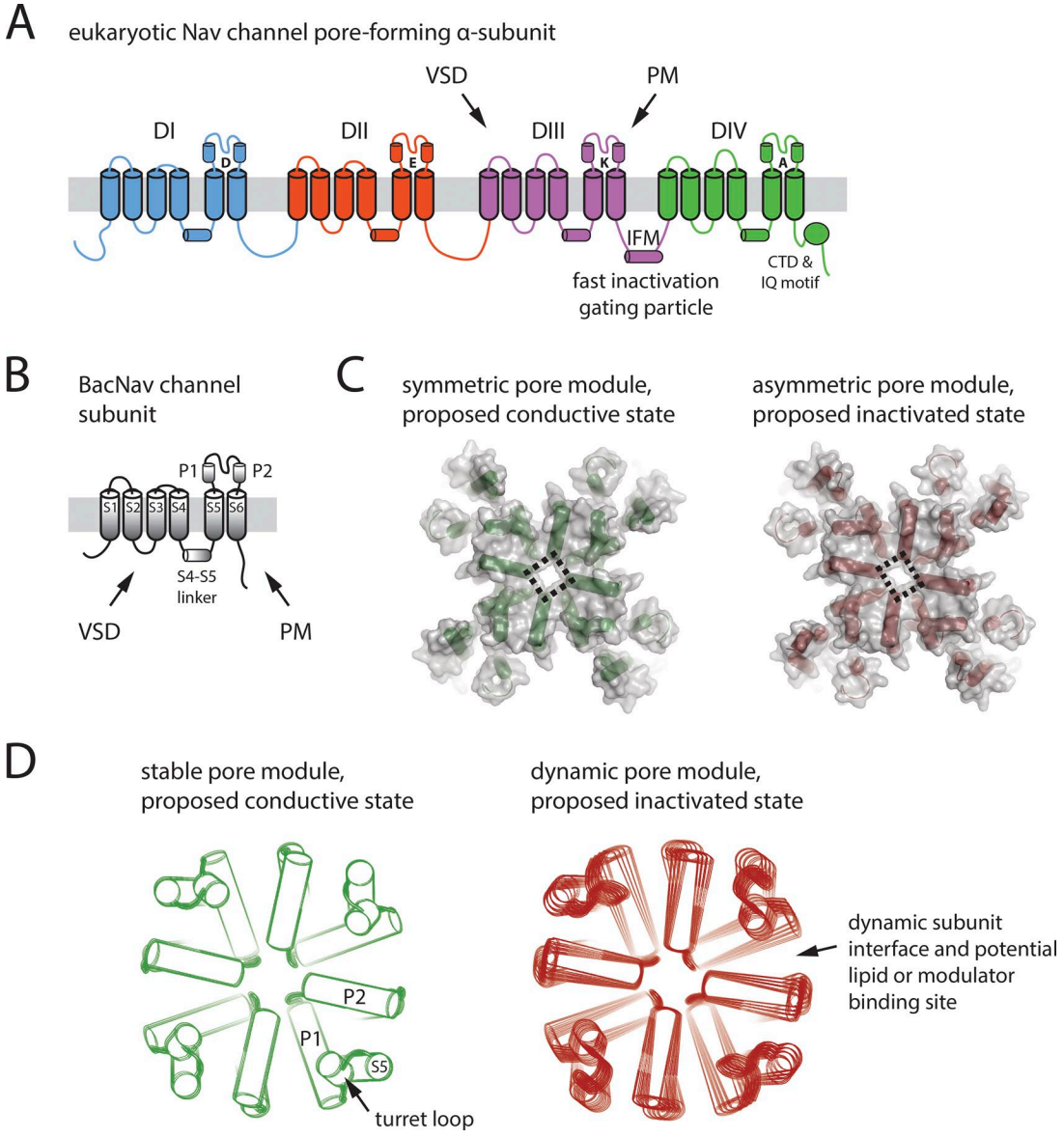

Figure 1. **Proposed structural features of conductive and inactivated bacterial Nav channel states. (A)** Schematic view of an eNav channel pore-forming α-subunit; β-subunits are not depicted for clarity. **(B)** Schematic view of a BacNav channel subunit. **(C)** Extracellular views of available BacNav channel crystal structures proposed to have selectivity filters captured in a conductive (green) or inactivated (red) state. Conductive selectivity filter structures are represented by $NavAb_{I217C}$ (PDB accession no. 3RVY, shown in green) or NavMs (PDB accession no. 5HVD); inactivated selectivity filter structures are represented by $NavAb_{WT}$ (PDB accession no. 4EKW, shown in red) or NavRh (PDB accession no. 4DXW). **(D)** Schematic summary of the results reported by Chatterjee et al. (2018) obtained from EPR and DEER studies on a panel of NavSp1 channel spin-labeled mutants. VSDs are not depicted for clarity as mutations studied in NavSp1 targeted the turret loop, P1 helix, and P2 helix. The authors proposed that a dynamic, asymmetric pore module represents the inactivated state (depicted in red), whereas a much less dynamic, more symmetric pore module represents the conductive state (depicted in green).

that actually prevent Na^+ conductance within slow inactivated states remain poorly described. An important opportunity to begin to unveil the structural basis of slow inactivation in Nav channels arrived with the molecular characterization of NaChBac from *Bacillus halodurans*, the first cloned BacNav channel (Ren et al., 2001).

Unlike eNav channels, BacNav channels are homotetramers formed from a single six transmembrane segment–containing subunit (Fig. 1, B and C; Payandeh and Minor, 2015). However, BacNav channels share several key functional properties with eNav channels, including voltage-dependent activation, Na^+ selectivity, inactivation, and sensitivity to pore-blocking drugs (Ren et al., 2001). It has been assumed that inactivation in BacNav channels is analogous to slow inactivation in eNav channels, in part because BacNav channels lack sequences that resemble the intracellular DIII-DIV linker required for fast inactivation (Fig. 1, A and B; Ren et al., 2001). Consistent with these assumptions, mutations within the PM, VSD, and intracellular domain can impact the kinetics and voltage-dependence of inactivation in BacNav channels (Pavlov et al., 2005; Irie et al., 2010; Gamal El-Din et al., 2013; Arrigoni et al., 2016). Inactivation is also a multistate process in BacNav channels (Gamal El-Din et al., 2013), which is

reminiscent of eNav channels, where the presence of multiple and physically distinct slow inactivated states is thought to depend on the duration or frequency of depolarization (Vilin and Ruben, 2001; Silva, 2014). High-resolution crystal structures of BacNav channels are now available in symmetric (NavAb and NavMs) and asymmetric (NavAb and NavRh) conformations, which have been interpreted as potentially different functional channel states (Fig. 1 C; Payandeh et al., 2011, 2012; Zhang et al., 2012; Sula et al., 2017). Together with the available structural information, Chatterjee et al. (2018) took advantage of the large (milligram) quantities of full-length recombinant proteins that can be generated for thorough biophysical analysis of BacNav channels. Following previous reports (Shaya et al., 2011), the authors also produced PM-only BacNav channel proteins that are completely freed from their VSDs (Chatterjee et al., 2018).

Chatterjee et al. (2018) focused on the NavSp1 channel from the bacterium *Silicibacter pomeroyi* (Shaya et al., 2011) to investigate the conformational changes within the selectivity filter region during inactivation. Because full-length NavSp1 channels are expected to be predominately in inactivated conformations under steady-state conditions at 0 mV, Chatterjee et al. (2018) additionally used a PM-only construct as a surrogate for the conductive conformation after confirming that it opens stochastically and is less prone to inactivation in the absence of VSDs. Using recombinant protein production in conjunction with site-directed spin labeling, liposome reconstitution, and EPR spectroscopy, Chatterjee et al. (2018) systematically mapped out differences in spin-label dynamics and solvent accessibility across the full-length and PM-only NavSp1 channel constructs. Using double electron-electron resonance (DEER) spectroscopy distance measurements, the authors also quantified the extent of conformational changes underlying NavSp1 inactivation, and their collective results are quite illuminating.

The methods employed by Chatterjee et al. (2018) are biophysical approaches that can return site-specific structural and dynamic information from detergent-solubilized or liposome-reconstituted membrane proteins. An appropriate EPR spin label was first incorporated site-specifically into the NavSp1 channel protein after cysteine mutagenesis and recombinant protein purification. After separation from unreacted spin label, Chatterjee et al. (2018) reconstituted the full-length and PM-only NavSp1-labeled proteins into liposomes composed of asolectin lipids. The key to EPR spectroscopy is that the spin label produces an absorption spectrum that is sensitive to its physical environment. In that way, when coupled to scanning mutagenesis and reiterative EPR measurements, a residue-level plot of probe dynamics, solvent exposure, and lipid exposure can be mapped onto available structural models of the channel protein. Notably, spin probe dynamics are governed by local steric contacts as well as the flexibility of the protein backbone to which it is attached. Additionally, DEER spectroscopy is a form of pulsed EPR experiments that can estimate inter-probe distances to provide information about the symmetry (or asymmetry) experienced by the four spin labels on each homotetrameric NavSp1 channel. Because technical complications arise for liposome-reconstituted samples, one caveat of the work is that detergent-solubilized NavSp1-labeled samples were used for DEER experiments. Nevertheless, the impressive power of the methods employed by Chatterjee et al. (2018) come to light as they generate and study >30 spin-labeled NavSp1 channel variants as both full-length and PM-only proteins, so this work represents a technical tour de force.

Chatterjee et al. (2018) began their study by probing an S6 position near the intracellular activation gate in the PM-only NavSp1 construct to demonstrate that EPR and DEER measurements are inconsistent with a closed activation gate, but better match with expectations for a conductive activation gate. Hence, the authors confirmed that the NavSp1 PM-only channel construct can serve as a proxy for the open or conductive state (Shaya et al., 2011). Chatterjee et al. (2018) then systematically scanned the turret loop, the P1 helix, and the P2 helix of the full-length (i.e., inactivated) and PM-only (i.e., conductive) channel proteins, and observed some remarkable differences that suggest the structure of the selectivity filter region is substantially different between the inactivated and conductive channel conformations. In general, probes incorporated into full-length NavSp1 channels were more mobile than those in the PM-only channels, suggesting that the extracellular pore region is much more dynamic in the inactivated state. Therefore, a key conclusion of this study is that the outer pore region of NavSp1 becomes dynamic in the inactivated state (Fig. 1 D), which is surprising considering that slow inactivated states in eNav channels are often assumed to be quite stable. However, a dynamic selectivity filter region in the inactivated state seems consistent with prior physiological results demonstrating that permeant ions and TTX slow entry into, and enhance recovery from, slow inactivated states, presumably by stabilizing a conductive conformation of the selectivity filter (Townsend and Horn, 1997; Cervenka et al., 2010).

The EPR spectra that Chatterjee et al. (2018) obtained for their full-length NavSp1 samples also reveal two distinct components, which could arise because of asymmetry within the inactivated channels. A departure from symmetry was previously reported for potentially inactivated state structures of NavAb and NavRh (Fig. 1 C; Payandeh et al., 2012; Zhang et al., 2012). However, the data from Chatterjee et al. (2018) suggest much more dramatic differences occurring within the outer pore region of NavSp1 compared with available NavAb structures, perhaps because the NavAb crystal lattice selects for only a subset of potential channel structures along the inactivated state ensemble (Payandeh et al., 2012). It is interesting that residues which line the NavSp1 intersubunit interface within the outer pore region are the most mobile within the inactivated state, especially because the architecture of this interface is distinct from that found in K^+ channels. The dynamic PM interface identified within the inactivated NavSp1 channels is also directly exposed to the membrane bilayer, where a well-resolved lipid has repeatedly been seen to bind in emerging Nav, Cav, and TRP channel structures (Fig. 1 D; Payandeh et al., 2011; Gao et al., 2016; Tang et al., 2016; Wu et al., 2016). It should not escape attention that the dynamic P1 and P2 helix intersubunit interface identified by Chatterjee et al. (2018) directly abuts an ultra-conserved membrane-facing tryptophan residue present in all BacNav channels (Payandeh and Minor, 2015), or that this dynamic interface delineates a membrane-exposed binding site for therapeutically relevant channel modulators (Fig. 1 D; Tang et al., 2016). Collectively, the evidence makes it hard to suggest that

the work of Chatterjee et al. (2018) represents an esoteric finding only pertinent to NavSp1 or BacNav channels, and it is perhaps easier to speculate that this study highlights a dynamic site of channel modulation and inactivation that is conserved across the Nav channel superfamily, and possibly beyond.

To evaluate the potential relevance of the dynamic PM intersubunit interface, Chatterjee et al. (2018) mutated a residue in NavSp1 that is analogous to a known Nav1.5 disease-causing mutation and found enhanced use-dependent inactivation and a left shift in the voltage dependence of steady-state inactivation. The authors further reconstituted select full-length NavSp1 channels into DOTAP (1,2-dioleoyl-3-trimethylammonium propane), a lipid suggested to promote the deactivated state of VSDs, and indeed observed marked similarities to the EPR spectra of matched conductive PM-only NavSp1 samples. Chatterjee et al. (2018) suggest that the VSDs may operate allosterically through the PM to impart voltage-dependence of inactivation, but this remains an open question for future investigation. Similarly, Chatterjee et al. (2018) do not report the consequences of increasing (or decreasing) permeant ion concentrations, the effect that local anesthetics may induce within the full-length and PM-only channel constructs, or mutation of the highly conserved S6 asparagine known to impact slow inactivation in eNav channels. Although rigorous and thorough, an inescapable limitation of the current work is that NavSp1 only represents a model system to study inactivation; therefore, this type of evaluation will need to be transferred to a bona fide eNav channel before we might understand the impact of channel modulation by phosphorylation, calmodulin, toxins, or human disease mutations on outer pore dynamics and slow inactivation. Still, this groundbreaking study by Chatterjee et al. (2018) clearly sets the stage for many more intriguing investigations, and my hope is that these follow-on studies will not be slow to develop.

Acknowledgments

J. Payandeh is an employee of Genentech, Inc; J. Payandeh also acknowledges Oliver, Naomi, and Emily Payandeh for their continued support and help to generate Figure 1.

Merritt C. Maduke served as editor.

References

Ahern, C.A., J. Payandeh, F. Bosmans, and B. Chanda. 2016. The hitchhiker's guide to the voltage-gated sodium channel galaxy. *J. Gen. Physiol.* 147:1–24. https://doi.org/10.1085/jgp.201511492

Armstrong, C.M., F. Bezanilla, and E. Rojas. 1973. Destruction of sodium conductance inactivation in squid axons perfused with pronase. *J. Gen. Physiol.* 62:375–391. https://doi.org/10.1085/jgp.62.4.375

Arrigoni, C., A. Rohaim, D. Shaya, F. Findeisen, R.A. Stein, S.R. Nurva, S. Mishra, H.S. Mchaourab, and D.L. Minor Jr. 2016. Unfolding of a Temperature-Sensitive Domain Controls Voltage-Gated Channel Activation. *Cell.* 164:922–936. https://doi.org/10.1016/j.cell.2016.02.001

Capes, D.L., M.P. Goldschen-Ohm, M. Arcisio-Miranda, F. Bezanilla, and B. Chanda. 2013. Domain IV voltage-sensor movement is both sufficient and rate limiting for fast inactivation in sodium channels. *J. Gen. Physiol.* 142:101–112. https://doi.org/10.1085/jgp.201310998

Cervenka, R., T. Zarrabi, P. Lukacs, and H. Todt. 2010. The outer vestibule of the Na+ channel-toxin receptor and modulator of permeation as well as gating. *Mar. Drugs.* 8:1373–1393. https://doi.org/10.3390/md8041373

Chatterjee, S., R. Vyas, S.V. Chalamalasetti, I.D. Sahu, J. Clatot, X. Wan, G.A. Lorigan, I. Deschênes, and S. Chakrapani. 2018. The voltage-gated sodium channel pore exhibits conformational flexibility during slow inactivation. *J. Gen. Physiol.*:jgp.201812118. https://doi.org/10.1085/jgp.201812118

Gamal El-Din, T.M., G.Q. Martinez, J. Payandeh, T. Scheuer, and W.A. Catterall. 2013. A gating charge interaction required for late slow inactivation of the bacterial sodium channel NavAb. *J. Gen. Physiol.* 142:181–190. https://doi.org/10.1085/jgp.201311012

Gao, Y., E. Cao, D. Julius, and Y. Cheng. 2016. TRPV1 structures in nanodiscs reveal mechanisms of ligand and lipid action. *Nature.* 534:347–351. https://doi.org/10.1038/nature17964

Hille, B. 1977. Local anesthetics: hydrophilic and hydrophobic pathways for the drug-receptor reaction. *J. Gen. Physiol.* 69:497–515. https://doi.org/10.1085/jgp.69.4.497

Irie, K., K. Kitagawa, H. Nagura, T. Imai, T. Shimomura, and Y. Fujiyoshi. 2010. Comparative study of the gating motif and C-type inactivation in prokaryotic voltage-gated sodium channels. *J. Biol. Chem.* 285:3685–3694. https://doi.org/10.1074/jbc.M109.057455

Kellenberger, S., T. Scheuer, and W.A. Catterall. 1996. Movement of the Na+ channel inactivation gate during inactivation. *J. Biol. Chem.* 271:30971–30979. https://doi.org/10.1074/jbc.271.48.30971

Pavlov, E., C. Bladen, R. Winkfein, C. Diao, P. Dhaliwal, and R.J. French. 2005. The pore, not cytoplasmic domains, underlies inactivation in a prokaryotic sodium channel. *Biophys. J.* 89:232–242. https://doi.org/10.1529/biophysj.104.056994

Payandeh, J., and D.L. Minor Jr. 2015. Bacterial voltage-gated sodium channels (BacNa(V)s) from the soil, sea, and salt lakes enlighten molecular mechanisms of electrical signaling and pharmacology in the brain and heart. *J. Mol. Biol.* 427:3–30. https://doi.org/10.1016/j.jmb.2014.08.010

Payandeh, J., T. Scheuer, N. Zheng, and W.A. Catterall. 2011. The crystal structure of a voltage-gated sodium channel. *Nature.* 475:353–358. https://doi.org/10.1038/nature10238

Payandeh, J., T.M. Gamal El-Din, T. Scheuer, N. Zheng, and W.A. Catterall. 2012. Crystal structure of a voltage-gated sodium channel in two potentially inactivated states. *Nature.* 486:135–139. https://doi.org/10.1038/nature11077

Ren, D., B. Navarro, H. Xu, L. Yue, Q. Shi, and D.E. Clapham. 2001. A prokaryotic voltage-gated sodium channel. *Science.* 294:2372–2375. https://doi.org/10.1126/science.1065635

Shaya, D., M. Kreir, R.A. Robbins, S. Wong, J. Hammon, A. Brüggemann, and D.L. Minor Jr. 2011. Voltage-gated sodium channel (Na_V) protein dissection creates a set of functional pore-only proteins. *Proc. Natl. Acad. Sci. USA.* 108:12313–12318. https://doi.org/10.1073/pnas.1106811108

Silva, J. 2014. Slow inactivation of Na(+) channels. *Handb. Exp. Pharmacol.* 221:33–49. https://doi.org/10.1007/978-3-642-41588-3_3

Sula, A., J. Booker, L.C. Ng, C.E. Naylor, P.G. DeCaen, and B.A. Wallace. 2017. The complete structure of an activated open sodium channel. *Nat. Commun.* 8:14205. https://doi.org/10.1038/ncomms14205

Tang, L., T.M. Gamal El-Din, T.M. Swanson, D.C. Pryde, T. Scheuer, N. Zheng, and W.A. Catterall. 2016. Structural basis for inhibition of a voltage-gated Ca2+ channel by Ca2+ antagonist drugs. *Nature.* 537:117–121. https://doi.org/10.1038/nature19102

Townsend, C., and R. Horn. 1997. Effect of alkali metal cations on slow inactivation of cardiac Na+ channels. *J. Gen. Physiol.* 110:23–33. https://doi.org/10.1085/jgp.110.1.23

Vilin, Y.Y., and P.C. Ruben. 2001. Slow inactivation in voltage-gated sodium channels: molecular substrates and contributions to channelopathies. *Cell Biochem. Biophys.* 35:171–190. https://doi.org/10.1385/CBB:35:2:171

West, J.W., D.E. Patton, T. Scheuer, Y. Wang, A.L. Goldin, and W.A. Catterall. 1992. A cluster of hydrophobic amino acid residues required for fast Na(+)-channel inactivation. *Proc. Natl. Acad. Sci. USA.* 89:10910–10914. https://doi.org/10.1073/pnas.89.22.10910

Woronzow, D.S. 1924. Über die Einwirkung des konstanten Stromes auf den mit Wasser, Zuckerlösung, Alkali- und Erdalkalichloridlösungen behandelten Nerven. *Pflugers Arch. Gesamte Physiol. Menschen Tiere.* 203:300–318. https://doi.org/10.1007/BF01722437

Wu, J., Z. Yan, Z. Li, X. Qian, S. Lu, M. Dong, Q. Zhou, and N. Yan. 2016. Structure of the voltage-gated calcium channel Ca(v)1.1 at 3.6Å resolution. *Nature.* 537:191–196. https://doi.org/10.1038/nature19321

Yan, Z., Q. Zhou, L. Wang, J. Wu, Y. Zhao, G. Huang, W. Peng, H. Shen, J. Lei, and N. Yan. 2017. Structure of the Nav1.4-β1 Complex from Electric Eel. *Cell.* 170:470–482.e11. https://doi.org/10.1016/j.cell.2017.06.039

Zhang, X., W. Ren, P. DeCaen, C. Yan, X. Tao, L. Tang, J. Wang, K. Hasegawa, T. Kumasaka, J. He, et al. 2012. Crystal structure of an orthologue of the NaChBac voltage-gated sodium channel. *Nature.* 486:130–134. https://doi.org/10.1038/nature11054